Molecular Therapy
Original Article

Amelioration of Neurosensory Structure and Function in Animal and Cellular Models of a Congenital Blindness

Ji Yun Song,[1] Puya Aravand,[1,10] Sergei Nikonov,[1,2,10] Lanfranco Leo,[1] Arkady Lyubarsky,[1,2] Jeannette L. Bennicelli,[1] Jieyan Pan,[1] Zhangyong Wei,[1] Ivan Shpylchak,[1] Pamela Herrera,[1] Daniel J. Bennett,[1] Nicoletta Commins,[1] Albert M. Maguire,[1] Jennifer Pham,[1] Anneke I. den Hollander,[3,4,5] Frans P.M. Cremers,[4,5] Robert K. Koenekoop,[6] Ronald Roepman,[4,7] Patsy Nishina,[8] Shangzhen Zhou,[1] Wei Pan,[2,8] Gui-shuang Ying,[2,9] Tomas S. Aleman,[1] Jimmy de Melo,[1] Ilan McNamara,[1] Junwei Sun,[1] Jason Mills,[1] and Jean Bennett[1,2]

[1]Center for Advanced Retinal and Ocular Therapeutics (CAROT) and F.M. Kirby Center for Molecular Ophthalmology, Scheie Eye Institute, University of Pennsylvania Perelman School of Medicine, Philadelphia, PA, USA; [2]Penn Vision Research Center, University of Pennsylvania Perelman, Philadelphia, PA, USA; [3]Department of Ophthalmology, Radboud University Medical Center, Nijmegen, the Netherlands; [4]Department of Human Genetics, Radboud University Medical Center, Nijmegen, the Netherlands; [5]Donders Institute for Brain, Cognition and Behaviour, Radboud University Nijmegen, Nijmegen, the Netherlands; [6]McGill Ocular Genetics Center, McGill University Health Center, Montreal, QC, Canada; [7]Radboud Institute for Molecular Life Sciences, Radboud University Medical Center, Nijmegen, the Netherlands; [8]The Jackson Laboratory, Bar Harbor, ME, USA; [9]Center for Preventive Ophthalmology and Biostatistics, University of Pennsylvania Perelman School of Medicine, Philadelphia, PA, USA

Most genetically distinct inherited retinal degenerations are primary photoreceptor degenerations. We selected a severe early onset form of Leber congenital amaurosis (LCA), caused by mutations in the gene *LCA5*, in order to test the efficacy of gene augmentation therapy for a ciliopathy. The *LCA5*-encoded protein, Lebercilin, is essential for the trafficking of proteins and vesicles to the photoreceptor outer segment. Using the AAV serotype AAV7m8 to deliver a human *LCA5* cDNA into an *Lca5* null mouse model of LCA5, we show partial rescue of retinal structure and visual function. Specifically, we observed restoration of rod-and-cone-driven electroretinograms in about 25% of injected eyes, restoration of pupillary light responses in the majority of treated eyes, an ~20-fold decrease in target luminance necessary for visually guided behavior, and improved retinal architecture following gene transfer. Using *LCA5* patient-derived iPSC-RPEs, we show that delivery of the *LCA5* cDNA restores lebercilin protein and rescues cilia quantity. The results presented in this study support a path forward aiming to develop safety and efficacy trials for gene augmentation therapy in human subjects with *LCA5* mutations. They also provide the framework for measuring the effects of intervention in ciliopathies and other severe, early-onset blinding conditions.

INTRODUCTION

Leber congenital amaurosis (LCA; OMIM: 204000) is one of the most severe groups of heritable blinding diseases. LCA is rare, occurring in 1:50,000 individuals, and is usually inherited in an autosomal-recessive fashion. LCA can be caused by mutations in any of at least 25 different genes (https://sph.uth.edu/RetNet/sum-dis.htm). Clinical features include severely abnormal vision, often detected within the first year of life, nystagmus, and progressive loss of what poor vision existed in early childhood. Clinical testing typically reveals severely abnormal or extinguished electroretinograms (ERGs), amaurotic pupils, reduced light sensitivity, and pigmentary changes in the retina.

LCA resulting from mutations in *RPE65*[1,2] has been the focus of multiple gene augmentation therapy clinical trials. Using adeno-associated virus serotype 2 (AAV2) as a delivery vector, several groups have shown that transduction of retinal pigmented epithelial (RPE) cells with a wild-type (WT) copy of the *RPE65* gene is both safe and can reverse many of the LCA disease symptoms.[3–8] A randomized, multi-center phase 3 study testing AAV2.*hRPE65*v2 (generic name, voretigene neparvovec-rzyl, Spark Therapeutics, Philadelphia, PA) has shown that subretinal (SR) injection of this therapeutic entity results in improvements in light sensitivity, visual field, and the ability to accurately and quickly navigate a course using visual cues over a range of luminance conditions.[9] The US Food and Drug Administration (FDA) granted drug approval for voretigene neparvovec-rzyl on December 19, 2017, making this one of the first approved gene therapy drugs in the USA.

Received 17 July 2017; accepted 18 March 2018;
https://doi.org/10.1016/j.ymthe.2018.03.015.

[10]These authors contributed equally to this work.

Correspondence: Jean Bennett, Center for Advanced Retinal and Ocular Therapeutics (CAROT), University of Pennsylvania Perelman School of Medicine, 309C Stellar-Chance Labs, 422 Curie Blvd., Philadelphia, PA 19104, USA.
E-mail: jebennet@pennmedicine.upenn.edu

The development of a gene therapy for retinal dystrophies caused by *RPE65* mutations has paved the way for new gene augmentation therapies targeting other early onset retinal degenerative diseases. Most of these diseases are caused by mutations in photoreceptor-specific expressed genes. One of the most severe forms of LCA is caused by mutations in the photoreceptor-expressed gene *LCA5*, which encodes the lebercilin protein.[10–17] *LCA5* is estimated to account for ~2% of LCA cases, although it may be more prevalent in populations that are genetically isolated.[15] *LCA5* mutations have also been shown to be causative in other early onset forms of retinal degeneration, including cone dystrophy and autosomal recessive retinitis pigmentosa (ARRP).[13,15,18]

Lebercilin is expressed widely during development and is found in cilia of cultured cells as well as in the connecting cilium of mature photoreceptor cells.[10–17] The connecting cilium is a narrow structure between the photoreceptor inner segment (IS) that harbors the biosynthetic machinery of the cell and the outer segments (OSs) that contain components of the opsin-driven visual cascade. The connecting cilium functions as a conduit, supporting the bi-directional trafficking of proteins and vesicles along ciliary microtubule tracks in a process known as intraflagellar transport (IFT). Applying quantitative affinity proteomics to a genetically engineered *Lca5* mouse model, Boldt et al.[19] demonstrated that *Lca5* loss of function disrupts IFT, thereby causing defects in photoreceptor OS development and failed arrestin and opsin trafficking. The *Lca5* null ($Lca5^{gt/gt}$) mice lack cone and rod ERG responses and undergo an early and progressive retinal degeneration with only a single row of dispersed nuclei (compared to 8–10 rows of contiguous cells in retinas of WT mice) present in the outer nuclear layer (ONL) by 2 months of age.[19]

Development of a proof-of-concept for gene augmentation therapy in the $Lca5^{gt/gt}$ mouse model entails several challenges: (1) because retinal degenerative changes begin very early and progresses rapidly, intervention must be carried out in neonatal mice; (2) since this is a photoreceptor-specific disease, recombinant AAV vectors must be employed that target photoreceptors efficiently. The AAV2 vector used extensively in animal and human studies to target RPE cells does not target photoreceptors as efficiently as other AAV serotypes as shown by transduction comparisons of different serotypes after infection with equivalent doses.[20,21] Ideally, therapeutics should be developed that could ultimately progress to human clinical trials; and (3) outcome measures must be developed that accurately identify and quantify improvements in retinal and visual function, which is so low at baseline that it is difficult to score. Here, we used a recombinant AAV vector (AAV7m8) designed by directed evolution[22] to deliver a codon-optimized human lebercilin-encoding cDNA. By using AAV7m8 to deliver *LCA5* to the diseased photoreceptors early in life, we show that gene augmentation therapy results in both structural improvement of the $Lca5^{gt/gt}$ mouse retina and functional improvement of its vision.

RESULTS

Characterization of Transduction Properties of a rAAV Delivering WT *LCA5*

A recombinant (r)AAV vector, AAV7m8.CβA.hopt-*LCA5*, was generated, which delivered a codon-optimized human *LCA5* cDNA under the control of a hybrid chicken beta-actin (CβA) promoter with a cytomegalovirus (CMV) immediate early enhancer (Figure 1A). Reporter vectors incorporated an EGFP cDNA in place of the hopt-*LCA5* cDNA. The AAV7m8.CβA.hopt-*LCA5* virus was able to drive efficient expression of the human *LCA5* transgene in mouse retina (Figures 1A and 1B) following both intravitreal (IVT) and SR administration (Figures 1C and 1D, respectively). Western blot analysis shows production of the predicted ~81-kDa LCA5 protein at post-natal day (P)20 after intra-ocular delivery with AAV7m8.CβA.hopt-*LCA5* in $Lca5^{gt/gt}$ and WT mice treated at P5 (Figure 1B). Immunofluorescence analysis shows presence of lebercilin protein in the ONL, ISs, and connecting cilia (CC) in WT adult retina (Figure 1E). After injecting AAV7m8.CβA.hopt-*LCA5* IVT or SR in $Lca5^{gt/gt}$ retinas, lebercilin is found in CC as well as IS and ONL (Figures 1G and 1H). In contrast, in sham-injected $Lca5^{gt/gt}$ retina, there is no lebercilin (Figure 1F). In addition, after IVT injection, a substantial number of Müller cells produce lebercilin (Figure 1G).

Electroretinography: Retinal and Visual Function Improvements after Delivery of AAV7m8.CβA.hopt-*LCA5* to the $Lca5^{gt/gt}$ Retina

We recorded ERGs from eight $Lca5^{gt/gt}$ mice, five WT animals, and 16 $Lca5^{gt/gt}$ mice whose left eyes had been injected with excipient and the right eyes with AAV7m8.CβA.hopt-*LCA5* on P5 IVT. None of the eyes of $Lca5^{gt/gt}$ uninjected controls or $Lca5^{gt/gt}$ eyes injected with excipient (a total of 32 eyes) produced detectable ERG responses. Out of 16 eyes injected with AAV7m8.CβA.hopt-LCA5, four showed ERG responses to dim flashes of light in the dark-adapted state consistent with rod mediation of the signals, as well as mixed rod-cone responses to brighter flashes of light that resembled a smaller, scaled version of WT mixed rod-cone ERG waveforms (Figure S2). Light-adapted ERGs were also detectable in these eyes, suggesting cone mediation of the photopic responses. Detectable ERGs post-treatment ranged in amplitude from 20% to 25% of the WT amplitudes (Figure S2). The results suggest restoration of both rod and cone photoreceptor function after gene therapy in some of the animals. The inconsistency of the full-field ERG findings likely reflects incomplete retinal coverage and/or tissue damage (cataracts, unresolved detachment, etc.) sustained after these technically challenging SR injections, performed in the early post-natal period. The results, however variable in magnitude or infrequent, were dramatically different from the undetectable ERGs observed in untreated $Lca5^{gt/gt}$ eyes.

MEA: Kinetics of the Response of the $Lca5^{gt/gt}$ Retina to IVT AAV7m8.CβA.hopt-*LCA5*

Light responses of five *Lca5gt/gt* retinas and animals after IVT delivery of AAV7m8.CβA.hopt-*LCA5* at P5 were probed using multi-electrode array (MEA) analyses. The rationale for using MEA

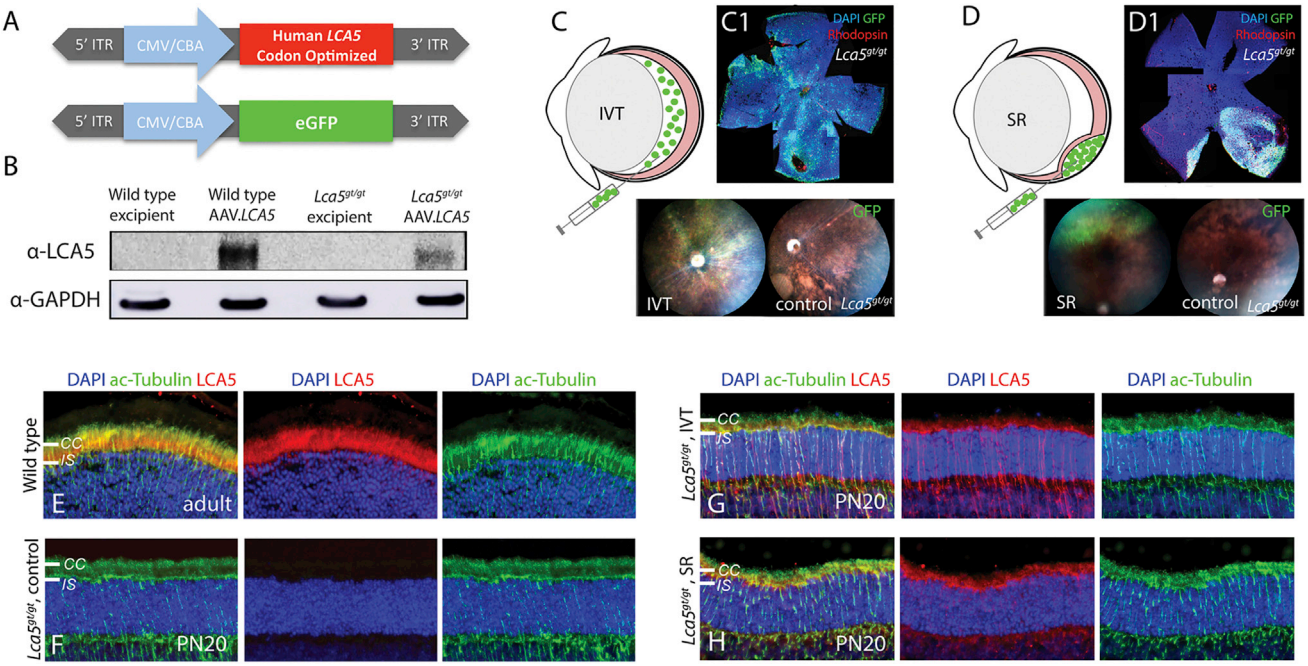

Figure 1. Transgene Cassettes and Transgene Expression

(A) Transgene cassettes used to generate AAV7m8.CβA.hopt-LCA5 and AAV7m8.CβA.eGFP; (B) western blot analysis shows production of the 81-kDa *LCA5*-encoded (Lebercilin) protein after delivering 9.2E+09 – 1.05E+10 vg/μL of AAV7m8.CβA.hopt-LCA5 into wild-type (WT) or $Lca5^{gt/gt}$ mouse retina, intravitreally. (C) Schematic drawings of intravitreal (IVT) and (D) subretinal (SR) injection adjacent to representative whole-mount micrographs of (C1) post-natal day (P)5 IVT-injected and (D1) P5 SR-injected retinas showing GFP expression. (E–H) Immunofluorescence analysis of LCA5 (red) and acetylated tubulin (green) in retinas from WT (adult) (E), control (sham-injected) $Lca5^{gt/gt}$ (F), P5 AAV7m8.CβA.hopt-*LCA5* IVT-injected (G), and SR-injected $Lca5^{gt/gt}$ (H) eyes harvested at P20. (G and H) In treated retinas, LCA5 (red) is produced mainly in inner segment (IS) and CC. (F) In contrast, lebercilin is absent in control $Lca5^{gt/gt}$ retinas. OS, outer segment.

is that it measures the output signal of the retina sent to the brain and thus, in addition to testing photoreceptor function, also provides information about retinal wiring. Of the five retinas and animals tested with MEA, two had clearly detectable rod and cone ERGs (see a representative record in Figure S2), and from three others, ERGs were small or undetectable. Three out of five AAV7m8.CβA.hopt-*LCA5*-injected $Lca5^{gt/gt}$ retinas (including those from the two eyes which had generated ERGs) had strong MEA-measured light responses, one had median responses, and one had minimal response in MEA testing (Figure 2; Table S1). MEA responses became detectable at intensities as low as 42–112 hv $\mu m^{-2}s^{-1}$ (455 nm light), and strong responses were observed through the full range of intensities up to the brightest intensity of 2.00E+09 hv $\mu m^{-2}s^{-1}$ (Figure 2). If we assume (1) the collecting area for rods and cones for end-on illumination is around 1 μm^2 at the wavelength of peak sensitivity[23,24] (note that both in ERG and our MEA experiments, light enters the retina from the ganglion cell side) and (2) the efficiency of stimulation by 455 nm light of rhodopsin and of M- and S-cone opsins is around 60%, 50%, and 0.3%, respectively,[25–27] the dim light generating clearly detectable responses in our experiments should produce less than 70 photoisomerizations per second per cell in rods, less than 60 in M-cones, and around 0.3 photoisomerizations per second in S-cones. Data from suction pipette recording show that at this rate of pigment excitation, rods can generate detectable light responses (response amplitude above 20% of the maximum), while cone response is expected to be at least 20 times smaller under the most favorable conditions (dark adapted M-cones in rod-transducin knockout retinas) and should be undetectable in rod-dominated mouse retina[25,26,28] (note that collecting area for side-on illumination in suction pipette recording is around 0.5 μm^2 for rods and 0.2 μm^2 for cones). Thus, observation of light responses at the dimmer intensity range in our experiments indicates recovery of rod function in the treated $Lca5^{gt/gt}$ retinas. Responses at the brighter end of intensities should originate in cones (the brightest intensity should be more than capable of driving both M- and S-cones by producing around 1.00E+9 and 6.00E+6 photoisomerizations per second per cell in M- and S-cones, respectively). As expected for rod/cone-driven responses, after exposure to the brightest stimulation series at the end of the first intensity series run (light-sensitive retinas were subjected to at least two intensity series runs ranging from the dim scotopic to the brightest photopic intensities in ~0.5 log increments), scotopic responses disappeared, but photopic responses were not significantly affected (Figures 2C and 2D). WT and treated $Lca5^{gt/gt}$ retinas were also responsive to 4 Hz flicker stimulation at the intensities expected to drive cone responses (Figure S8).

Retinas from sham-injected eyes showed minimal to abolished responses with high spontaneous firing and prominent melanopsin

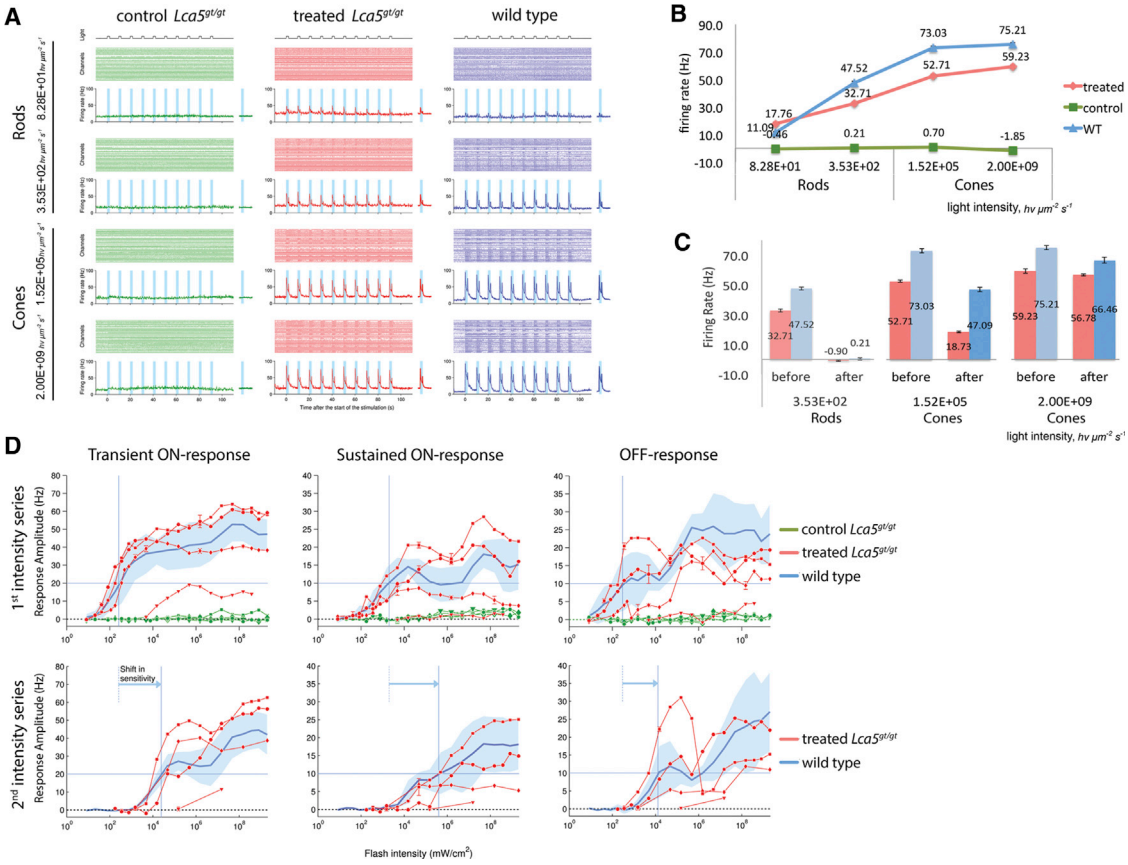

Figure 2. Multi-electrode Array Responses from *Lca5*$^{gt/gt}$ AAV7m8.hopt-*LCA5*-Treated Rods and Cones Are Similar to Those of Wild-Type Retinas

(A) Each row gives raster plots (each dot representing an action potential firing event, each dotted line corresponding to the multi-electrode array [MEA] channel) and per channel averaged firing rates (calculated using 100 ms time bin) obtained from untreated (green traces), treated (red traces), and wild-type (WT) (blue traces) retinas stimulated with a series of 10 flashes of particular intensity. Per flash averaged responses are shown to the right of the firing rate traces. Traces at the top and vertical blue shaded bars indicate light flashes. (B) Response amplitude (difference in firing rates before and after flash onset) versus flash intensity data measured from per flash averaged traces shown in (A). Responses from treated retinas are as high as 70% of the response from WT retina; there are minimal to abolished responses from untreated retina. (C) Response amplitudes from retinas of (A) for the first and second intensity series runs (before/during and after brightest exposures at the end of the first run; during each intensity series run, stimulation series intensity was increased from scotopic to the brightest photopic values in ~0.5 log increments). Error bars are ± SEM. (D) Amplitudes of transient ON (difference in firing rates before and after flash onset), sustained ON (difference before flash onset and offset), and OFF responses (difference before and after flash offset) as functions of the flash intensity for the first and second intensity series runs. Light-blue-shaded areas represent range of WT responses (four retinas, mean ± SD); blue traces give averaged WT response amplitudes. Horizontal arrows illustrate rightward shift in sensitivity caused by exposure to the brightest flashes at the end of the first intensity series run. Treated *Lca5*$^{gt/gt}$ and WT retinas show similar response/intensity dependencies before and after bleaching, while untreated *Lca5*$^{gt/gt}$ retina responses are flattened.

responses (Figures 2 and S9). Slow melanopsin-driven responses were also detected in both AAV7m8.CβA.hopt-*LCA5*-treated *Lca5*$^{gt/gt}$ retinas and retinas from WT mice (manifesting as elevated firing rate at the start of the second flash due to the slow recovery after the first flash in a series), although amplitudes of melanopsin response appears to be muted in treated retinas compared to the untreated ones.

Responses of treated and WT retinas had similar amplitude and intensity dependencies. One treated retina tested after the shortest post-injection period demonstrated reduced light sensitivity and absence of OFF and sustained ON responses (red downward triangles on Figure 2D). Development of the OFF responses appears to require longer time post-injection compared to the ON responses, consistent with increased variability in the OFF response amplitudes observed for the treated retinas. Function of all ganglion cell types identifiable in the WT retinas under full-field stimulation was detected in the *Lca5*$^{gt/gt}$ AAV-treated retinas after spike sorting (Figure S10).

Though results obtained with electroretinography and MEA experiments demonstrated restoration of rod and cone function in at least some animals, these methods were inadequate for assessment of intervention efficiency in a majority of animals, since only a quarter of treated mice produced useful ERG signals. Therefore, we based assessment of intervention efficacy on two additional approaches,

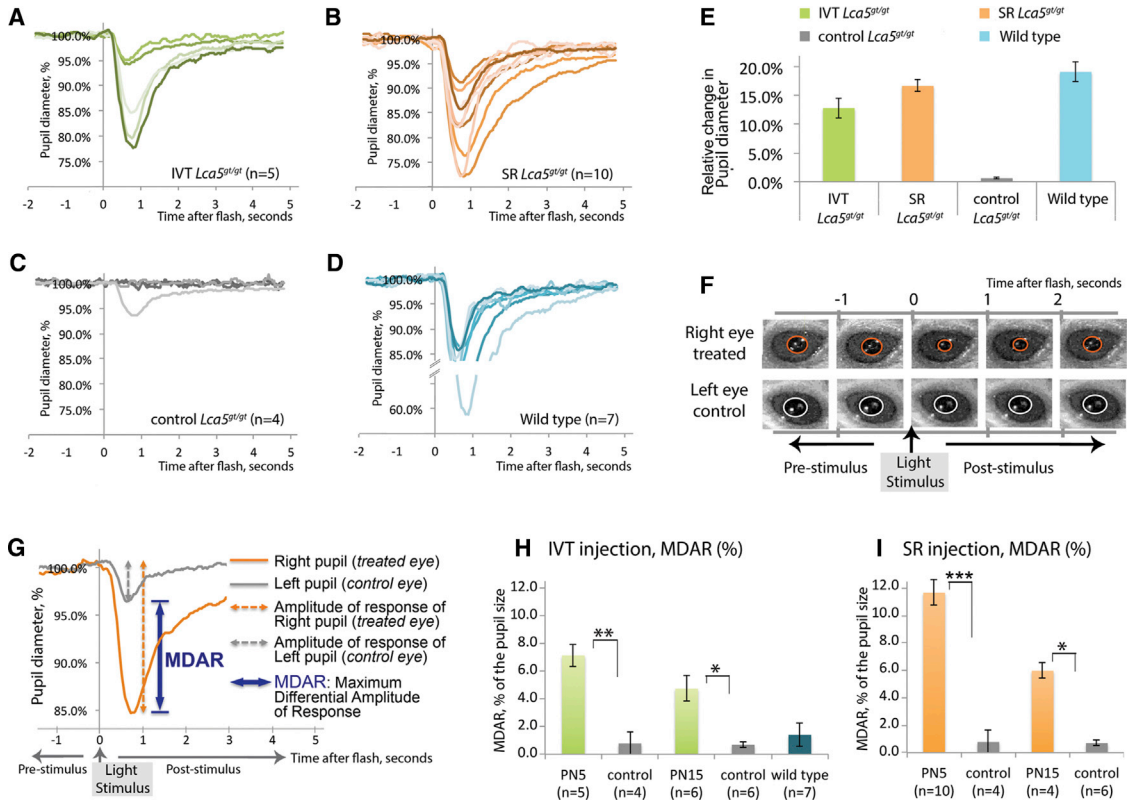

Figure 3. Normalized Pupillary Reflex Amplitudes of AAV7m8

CβA.hopt-*LCA5*-injected versus excipient-injected control eyes of *Lca5*$^{gt/gt}$ mice. Animals injected at post-natal days (P)5 and 15 were measured at 3 months of age using stimulation with 1K scot lux m^2 (for 40 ms). Results are shown after (A) intravitreal (IVT) and (B) subretinal (SR) injections, (C) in excipient-injected control *Lca5*$^{gt/gt}$ mice, and (D) in WT mice (C57BL/6). (E) Responses shown in (A)–(D) are summarized graphically. (F) Representative frames from video capture of pupils during the experiment; pupil area is marked in orange color for SR-injected right eye, and in white color for sham-injected left eye. (G) The maximum differential responses (MDAR) between right eye (treated with AAV7m8.hopt-*LCA5*) and left eye (sham-injected) control of one animal is shown. MDAR data from group analyses (the average responses) of (H) IVT-injected pupils and (I) SR-injected pupils at P5 or P15 are shown. *p < 0.1; **p < 0.05; ***p < 0.01. (E, H, and I) Error bars are ± SEM.

analyses of pupillary light reflexes (PLRs) and visual behavior, which offered, first, higher sensitivity than electrophysiology and, second, demonstration that treatment of the *Lca5*$^{gt/gt}$ retina with AAV7m8.CβA.hopt-*LCA5* results in light-induced signal relayed beyond the retina, through visual pathways to the brain.

PLRs are dependent upon relay of signals initially from photoreceptors to retinal ganglion cells, then to the Edinger-Westphal nucleus in the brain, and finally back to the pupillary sphincter muscle via the ciliary ganglion, which controls iris diameter. Analyses of the PLRs following stimulation of the treated versus control eyes revealed a significant ($p < 0.05$) increase in amplitude of the PLRs in eyes of *Lca5*$^{gt/gt}$ mice treated with AAV7m8.CβA.hopt-*LCA5* compared to sham-injected controls (Figure 3C). There was a significantly improved PLRs detected in animals injected at P5 either IVT or SR (Figures 3A, 3B, 3E, and 3F) such that near-WT responses were observed (Figure 3D). Statistically significant improvement of the amplitude of the PLRs was also demonstrated through comparisons of the maximum differential amplitude of response (MDAR; Figures 3G–3I and S1). Animals receiving AAV7m8.CβA.hopt-*LCA5* by either IVT or SR delivery also showed significantly improved PLRs as quantified by MDAR (Figures 3H and 3I).

Since PLRs demonstrate retinal signaling and function but do not provide information on formed vision, we used a light-cued water maze test to measure functional vision (Figure S3). The majority of untreated WT (normal-sighted) mice were able to navigate the water maze successfully at all light levels, whereas untreated *Lca5*$^{gt/gt}$ were severely impaired (Tables 1 and 2; Figure 4A). Results from water maze testing showed that both IVT and SR AAV7m8.CβA.hopt-*LCA5*-injected *Lca5*$^{gt/gt}$ animals performed better than uninjected controls in a statistically significant manner under at least one light condition (Tables 1 and 2; Figure 4). The animals treated SR at P5 showed a significantly improved pass rate at every lighting test condition (1.06E+05, 8.69E+03, and 5.87E+02 scot cd m^{-2}), than control excipient-injected cohort ($p < 0.01$). The decrease in target luminance necessary for visually guided behavior in treated animals was, as estimated from the horizontal shift of respective "light intensity versus

Table 1. Results of Water Maze Testing in *Lca5*$^{gt/gt}$ Mice: Intervention Type

		Mean (SD) for Pass %: Light Level (scot cd m^2)			
Intervention Type	n	1.06E+05	8.69E+03	5.87E+02	0
Excipient (PBS) intravitreal at P5	5	53.3 (36.36)	31.1 (9.29)	31.1 (21.38)	13.3 (9.29)
Excipient (PBS) intravitreal at P15	13	46.15 (17.5)	33.31 (17.57)	17.08 (9.74)	33.32 (13.64)
Excipient (PBS) subretinal at P5	7	73.0 (16.78)	34.9 (16.28)	22.2 (16.96)	14.3 (12.35)
AAV7m8-hopt-*LCA5* (+5% *eGFP*) intravitreal at P5	10	70.0 (17.43)	52.3 (13.93)	40.0 (21.09)	15.5 (13.03)
AAV7m8-hopt-*LCA5* (+5% *eGFP*) intravitreal at P15	13	53.85 (24.80)	28.19 (17.35)	18.78 (11.45)	27.75 (11.64)
AAV7m8-hopt-*LCA5* (+5% *eGFP*) subretinal at P5	17	88.9 (16.2)	77.1 (15.9)	47.7 (23.8)	14.4 (8.6)

Raw data: numbers of animals analyzed in each cohort and then tested under the designated light levels using the water maze.

Table 2. Results of Water Maze Testing in *Lca5*$^{gt/gt}$ Mice: Group Comparison

	p Value for Pairwise Comparison with PBS Control Group: Light Level (scot cd m^2)			
Group Comparison	1.06E+05	1.06E+05	1.06E+05	1.06E+05
AAV7m8-hopt-*LCA5* intravitreal at P5 versus excipient intravitreal at P5	0.24	0.01*	0.46	0.74
AAV7m8-hopt-*LCA5* intravitreal at P15 versus excipient intravitreal at P15	0.37	0.46	0.69	0.48
AAV7m8-hopt-*LCA5* subretinal at P5 versus excipient subretinal at P5	0.042*	0.00001*	0.018*	0.981

Note: Animals injected subretinally at P15 did not receive water maze testing. *Results of statistical analyses with $p \leq 0.05$.

success rate" plots in Figure 4C, ~20-fold. When animals were injected at P15 (IVT or SR), improvements were minimal (Figure 4). To confirm that mice used only the given light cue, testing was performed under no light condition (0.00 scot cd m^2) and over 90% of mice failed the test (including normal-sighted mice; Figure 4B).

Improvement in Retinal and Visual Function Correlates with Histologic Effects of *LCA5* Gene Transfer

Histologic rescue of *Lca5*$^{gt/gt}$ photoreceptors after treatment with AAV7m8.CβA.hopt-*LCA5* at P5 was assessed both through evaluation of molecules relevant to proper function of the phototransduction cascade and though structural measures.

Micrographs of H&E-stained retina showed that inner segments (ISs) and OSs and ONL are preserved through the 3 month time point (P99) after either IVT or SR injection of AAV7m8.hopt-*LCA5* (Figures 5A and 5B). In contrast, sham-injected control retinas lack such layers at P99 (Figure 5C). Further, lebercilin was detected in the treated, but not in sham-treated control retinas (Figures 5J and 5K). Persistent expression of rhodopsin in the ONL was also confirmed by immunofluorescence analysis (Figure S4) but only seen in treated eyes.

The thickness of photoreceptor cell layers in retinas that were treated by IVT or SR injection with AAV7m8.CβA.hopt-*LCA5* at P5 was significantly greater than in control retinas (Figure 5D). There was also a noticeable border in thickness between the areas of retinas exposed to or unexposed to AAV in retinas treated by SR injection (Figure S5). The preservation of photoreceptor layers persisted through the latest time point (P99). The increased thickness was due to an increased number of rows in the ONL and presence of ISs and OSs (Figures 5, S4, and S5). Consistent with this, there was a much higher proportion of dying photoreceptors in control compared to AAV.*LCA5*-treated retinas as judged by terminal deoxynucleotidyl transferase dUTP nick-end labeling (TUNEL) labeling, particularly within the first month after intervention (Figure S6).

Transmission electron microscopy confirms elaboration of OSs complete with stacked OS discs (Figures 5E and 5F), 9+0 microtubule arrays typical of primary cilia (Figure 5F) and CC (Figure 5G) after injection of AAV7m8.hopt-*LCA5* (Figures 5E–5G). There were no OS discs or CC identified in untreated mutant retinas (Figure 5H). The untreated retinas lack OSs and show massive degeneration of photoreceptors with only pyknotic nuclei and remnants of photoreceptor organelles.

Light stimulation of dark-adapted adult *Lca5*$^{gt/gt}$ retinas treated at P5 with AAV7m8.hopt-*LCA5* resulted in normal translocation patterns of phototransduction proteins into OSs. As shown in Figure S7, arrestin translocates properly after light exposure in AAV7m8.hopt-*LCA5*-treated retinas. Such activity could not be assessed in the control retinas due to the degeneration of ISs and OSs. The data reflect restoration of the IFT defect in the mouse retina after delivery of the WT *hLCA5* cDNA.

Preliminary Analysis of *LCA5* Disease in Humans

PLR testing was carried out to determine whether there was any evidence of function in the residual photoreceptors present in a human adult homozygous for *LCA5* mutations. As shown in Figure S11, PLRs were present in this individual with the same temporal sequence as those in a normal-sighted individual. However, the amplitudes of response were diminished considerably compared to the normal-sighted individual.

To aid in translating the mouse rescue studies to human, we studied human induced pluripotent stem cell (iPSC) lines that were generated for study from individuals with normal vision and those affected with LCA due to *LCA5* mutations. Recently, iPSC-derived retinal pigmented epithelium (RPE) has been shown to recapitulate the

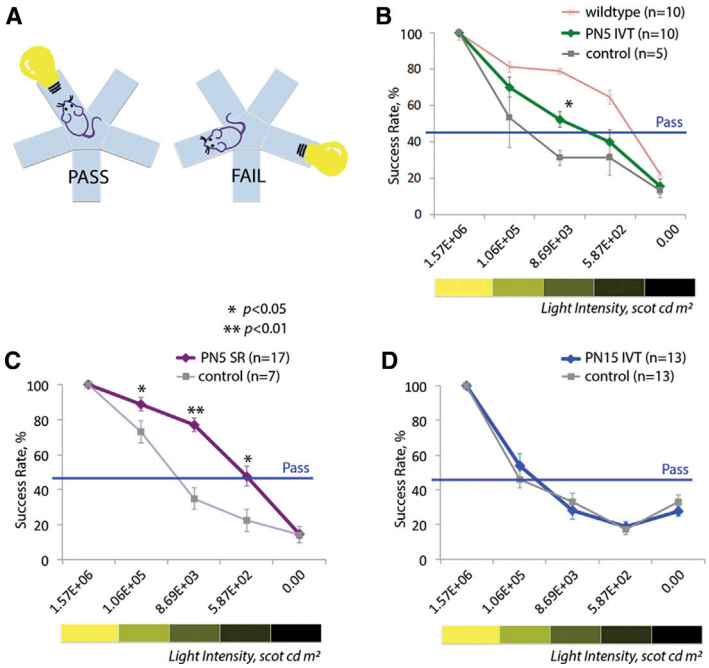

Figure 4. Water Maze Visual Behavior Test of AAV7m8.hopt-*LCA5*-Injected versus Excipient-Injected *Lca5*$^{gt/gt}$ Mice Treated at Post-natal Days 5 and 15 and Measured at 2.5 Months of Age

(A) Schematic of a 5-armed water maze, showing that there is a "pass" if the animal finds the lit platform and a "fail" if it does not. (B–D) The % success rate (pass rate) is plotted as a function of light intensity. "Light intensity" is defined as luminance of individual LEDs in the three LED light sources identifying the compartment with the escape platform (B) after intravitreal (IVT) or (C) sub-retinal (SR) injection at post-natal day (P)5. (D) Testing result after P15 IVT injection is compared. All left eyes were sham-injected. *p < 0.05; **p < 0.01. (B–D) Error bars are ± SEM.

functional phenotype of polarized epithelium, with secretion, gene expression, and maturation characteristics comparative to fetal and adult RPEs.[29] These cells show great promise for understanding disease mechanisms associated with defects in cilia biology.[30,31] Here, we differentiated iPSCs into RPE cells (Figure 6A), a process which allowed evaluation of ciliated cells in a shorter time span and more efficiently than if neuronal and photoreceptor cells had been generated (Figure S12). We evaluated *LCA5* gene expression and show that *LCA5* mRNA is expressed in unaffected iPSC-derived RPEs and the level of expression of *LCA5* in *LCA* patient-derived RPEs is significantly reduced compared to controls (Figure 6B). When ciliary distribution was measured, there were significantly fewer cilia present on the iPSC-RPE derived from the *LCA5* patient than on the RPEs from the normal-sighted individual (Figures 6D and 6E). Treatment of the *LCA5*-iPSC-RPE with AAV7m8.hopt-*LCA5* led to production of lebercilin protein (Figure 6C) and resulted in comparable cilia numbers in the AAV7m8.*LCA5* treated and normal-sighted individual RPE cells (Figures 6D–6F).

DISCUSSION

Retinal gene transfer using the most thoroughly studied recombinant AAV serotype, AAV2, has been carried out in >250 eyes in human subjects, and in 18 different clinical trials (https://clinicaltrials.gov).[32] These trials target diverse diseases, including autosomal defects (*RPE65* deficiency, retinitis pigmentosa due to *MERTK* mutations, choroideremia), a mitochondrial disease (Leber hereditary optic neuropathy), a complication of age-related macular degeneration (choroidal neovascularization), and end-stage retinal degeneration (using optogenetic therapy). In the majority of these studies, AAV2 was delivered SR in order to target RPE cells. The net result has been a large body of safety data with respect to SR delivery of AAV, the same surgical approach that will be necessary to target photoreceptors in patients with *LCA5* mutations.

While AAV2 vectors are capable of transducing photoreceptors, they do not do this as efficiently dose for dose as some other AAV serotypes. As mentioned above, photoreceptors comprise the primary cell type affected in LCA5 and most other inherited retinal degenerations. For this reason, we selected AAV7m8, a vector generated using a directed evolution approach.[22] AAV7m8 has been shown to target photoreceptors efficiently in both mice through either SR or IVT administration and in non-human primates (NHPs) using SR injection.[21,22] Here, we demonstrate that AAV7m8-mediated gene augmentation therapy with the *LCA5* cDNA in the neonatal *Lca5*$^{gt/gt}$ mouse can partially rescue retinal and visual function and also retinal structure.

The efficacy reported in this study includes amelioration of both rod and cone function as revealed by electroretinography and MEA experiments, improvements in the ability of treated animals to navigate using visual cues, restoration of visual pathways to the brain as shown by pupillometry, a reduction in photoreceptor apoptosis, and the preservation of functional photoreceptors with morphology and markers characteristic of this cell type, including presence of rhodopsin in the outer retina. The treated *Lca5*$^{gt/gt}$ photoreceptors show an increased thickness of ONLs with preserved OSs with stacked OS discs. This is in marked contrast to the untreated *Lca5*$^{gt/gt}$ retinas, which were reduced to a single row of non-contiguous photoreceptor nuclei by 3 months of age.[19] The improvements were not permanent. However, they persisted for at least 3 months at which point there are few remaining photoreceptors in the untreated *Lca5*$^{gt/gt}$ mouse. Electroretinography and MEA results show that with successful transduction of photoreceptors, *LCA5* gene therapy is capable of at least partially restoring responses mediated by both rod and cone photoreceptors. The responses of the cells have near-normal kinetics, including responses reflecting the activity of a variety of ganglion cell types as well as a reversal of the dominating melanopsin responses observed in the untreated *Lca5*$^{gt/gt}$ retinas. These results were complementary with the pupillometry and visual behavior findings and will provide the framework for future studies aiming to further characterize and optimize treatment effects (including studies

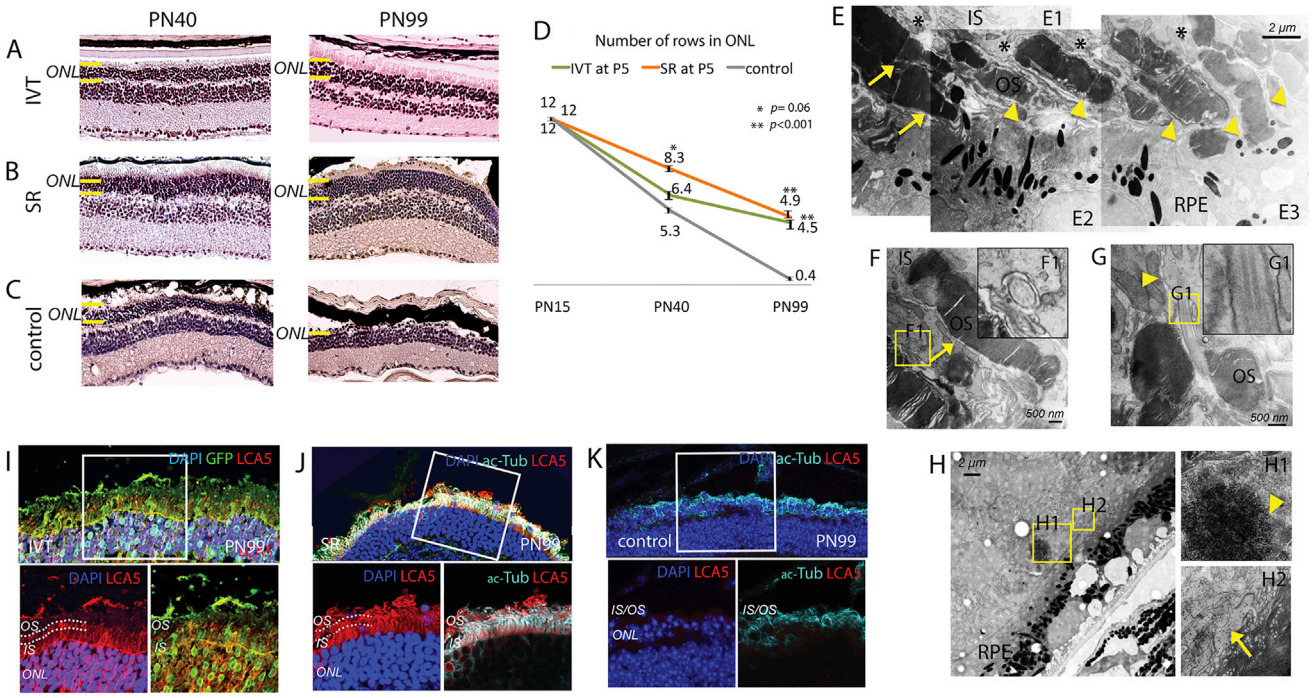

Figure 5. Representative Histology after AAV7m8.hopt-*LCA5* Delivery to the *Lca5*$^{gt/gt}$ Retina at Post-natal Day 5

(A–C) Comparing results of H&E-stain-treated and control retinal sections at P40 versus P99 after (A) intravitreal (IVT) or (B) subretinal (SR) injection of AAV7m8.hopt-*LCA5* (with 5% v/v AAV7m8.*eGFP*) compared with (C) sham injection. (D) Number of rows in the outer nuclear layer (ONL) after IVT or SR treatment with AAV.*LCA5* versus sham injection. Error bars are ± SEM. (E–H) Transmission electron microscopy (TEM) at P99 of retinas treated with (E–G) IVT AAV7m8.hopt-*LCA5* compared with (H) surgical sham. (E) Rod (arrowheads) and cone (arrows) photoreceptors have stacked outer segment (OS) discs and abundant mitochondria (*) in inner segments. (F) 9+0 microtubule array (F1, enlarged) and OS discs (arrows). (G) Connecting cilium (G1, enlarged) and basal body (arrowhead). (H) Pyknotic nuclei (H1, arrowhead) and (H2) remnants of rough endoplasmic reticulum (arrow) There are no OSs. RPE, retinal pigmented epithelium. (I) Lebercilin (red) in ONL and connecting cilium (between dotted lines) and IS of P5-treated retina at P99. (J and K) Co-labeling of lebercilin (red) with acetylated tubulin (cyan) appears white in SR-injected (J) versus untreated control (K) retinas at P99.

of visual behavior in low illuminance conditions). These data provide hope that a similar gene augmentation approach in humans as that used in the *Lca5*$^{gt/gt}$ mouse could result in improved vision. It may be possible to further optimize the intervention to obtain an even more durable rescue effect. Alteration of components of the transgene cassette (promoter, etc.) and areas of retina treated may lead to additional benefit. Dosing studies should identify the optimal dose for therapeutic effect.

The fact that *LCA5* null patients may retain photoreceptors through adulthood (whereas photoreceptors are lost early in life in mice) suggests that there may be a wider window of opportunity in *LCA5* humans compared to *Lca5* $^{gt/gt}$ mice. Photoreceptors have been documented in *LCA5* null humans in the foveal ONL, for up to 3 decades.[18,33] This is important since successful gene therapy requires that the affected cells be present. We were able to demonstrate that the retained photoreceptors in an adult with *LCA5* mutations showed a similar temporal pattern of light responsiveness (albeit reduced in amplitude), as photoreceptors from a normal-sighted individual. These results indicate that the residual photoreceptors in *LCA5* patients are functional, despite structural and physiological deficits. The primary cilia of iPSC-RPE derived from patients with *LCA5* mutations were much less numerous than those from the control cells. The facts that the ciliary defect in photoreceptors in the *Lca5*$^{gt/gt}$ mouse can be corrected by gene augmentation therapy and that the numbers of cells exhibiting cilia can be increased to normal levels suggest that it may be possible to ameliorate the ciliary defect present in humans with this condition.

This study marks the first step in planning to move forward to test for safety and efficacy of gene augmentation therapy in human subjects with *LCA5* mutations. There are a number of questions remaining that will need to be answered prior to embarking on a trial. For example, what is an appropriate dose to rescue effects resulting from the absence of Lebercilin in photoreceptors, and what are the consequences of delivering WT Lebercilin to other (non-photoreceptor) cells in the mature retina? In addition, there is a need to develop appropriate outcome measures for this severe blinding condition. One of the biggest questions in planning human clinical trials will be: what are the developmental constraints for achieving rescue? In the *Lca5*$^{gt/gt}$ mouse, we demonstrated rescue in both neonatal (P5) and juvenile (P15) mice. The greater extent of rescue apparent in P5 compared to P15 mice may be due to early photoreceptor loss in this mouse model. The failure of proper OS formation in the mouse model

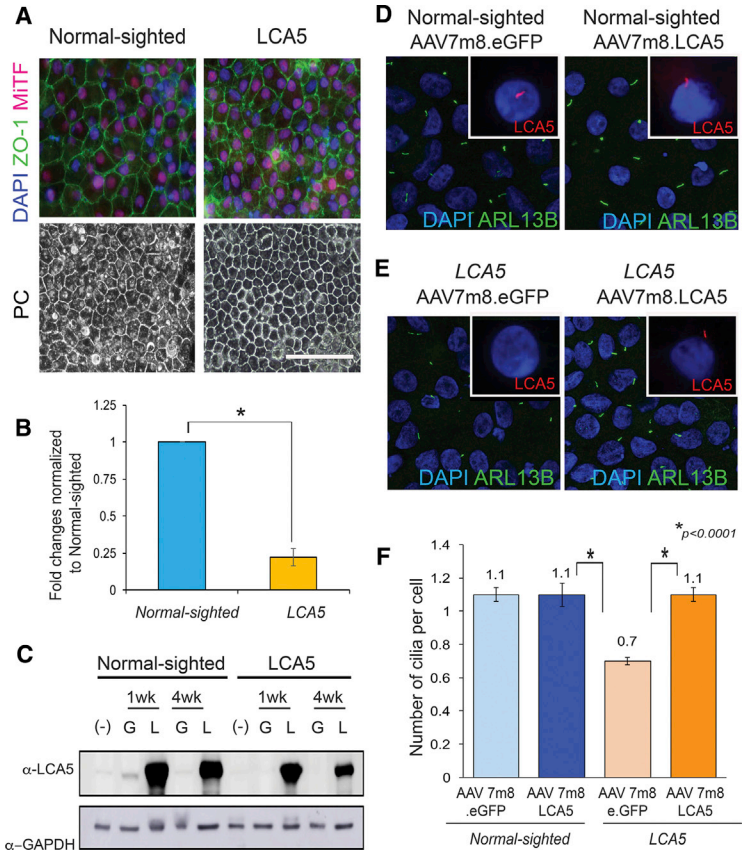

Figure 6. Cilia Phenotype Rescued in Homozygous Human *LCA5* p.(Q279*) iPSC-RPE after Treatment with AAV7m8.hopt-*LCA5*

(A) Confocal images show hexagonal morphology of mature RPE cells along with the immunofluorescently detectable RPE markers ZO-1 and MITF. Phase contrast (PC) images display the architecture of iPSC-RPE cultures of RPE derived from both a normal-sighted person and an *LCA5* patient. (B) qRT-PCR of *LCA5* mRNA expression in normal-sighted control RPEs and *LCA5* patient-derived RPEs. GAPDH is used to normalize expression levels. (C) Western blot analyses show endogenous (*) Lebercilin protein in normal-sighted control cells that are untreated ("−") or treated with AAV7m8.eGFP ("G"). There is no endogenous lebercilin in untreated or AAV7m8.GFP-treated *LCA5*-affected cells. There are robust levels of lebercilin after infection of cells from both normal-sighted and individuals with *LCA5* mutations with AAV7m8.*LCA5* ("L"). Immunofluorescence analyses show presence of Arl13b-positive primary cilia in normal-sighted (D) and LCA5-derived (E) iPSC-RPE. Lebercilin is present in normal-sighted control and AAV7m8.LCA5-treated (but not AAV7m8.eGFP-treated) *LCA5*-affected cells. (F) Quantitative analysis of number of cilia per cell in normal-sighted versus LCA5-iPSC-RPE shows rescue effect of cilia formation after treatment of LCA5-iPSC-RPE cells with AAV7m8.LCA5 (but not with AAV7m8.eGFP). Error bars are ± SD.

(coinciding with degeneration of photoreceptors)[19] implies that there are developmental components of the disease. There are likely developmental components in the human condition as well, for example, incomplete differentiation and a resultant impaired function of photoreceptors. The first step is to determine whether it is possible to improve the function of those photoreceptors. Whether the visual pathways can be resuscitated in humans with *LCA5* deficiency is another important question. A block in information flow from the retina to the brain early in life can limit the ability of the visual pathway to function later in life, even if the defect in the retina is repaired (e.g., amblyopia). A limited amount of function in childhood may, however, be sufficient to create a neural pathway that can be activated and mature later in life if the retinal defect can be corrected as shown in studies of humans severely visually impaired due to *RPE65* mutations. Those individuals enjoyed a partial reversal of their blindness (along with restoration of cortical vision and myelination of the retinal-cortical pathway corresponding with the treated portion of the retina) after retinal gene therapy, even though they had been blind for up to 3.5 decades prior to treatment.[4,34,35]

In summary, LCA is one of the most severe retinal degenerative diseases, and LCA caused by *LCA5* mutations is one of the most severe variants of this disease. Often patients bearing *LCA5* mutations only have light perception early in life. It is difficult to carry out structural studies and specialized tests of visual function in these ultra-low-vision subjects due to nystagmus. Thus, this disease is considered difficult to approach therapeutically and in terms of visual function study endpoints. However, the phenotype of the *Lca5*$^{gt/gt}$ mouse reflects many of the clinical findings in humans with *LCA5* variants. The rescue data in the *Lca5*$^{gt/gt}$ mouse provides the foundation for developing a gene augmentation approach that could result in improved vision in humans. Such an approach (using AAV7m8) would involve SR injection, since IVT injection of AAV7m8 does not result in efficient transduction of photoreceptors in large animal models (and presumably, humans).[20,21] While amelioration of the phenotype was observed after IVT injection of AAV7m8 in the mouse, it was not as efficient at rescuing the phenotype as SR injection. This may be due to the fact that the vector not only gets diluted after injection in the vitreous but is also exposed to many neighboring cell targets (ganglion cells, trabecular meshwork, anterior segment structures) that may bind it, thereby reducing exposure to the outer retina.

Additional studies in the *Lca5*$^{gt/gt}$ mouse can be used to optimize other variables that could affect efficacy and durability of a rescue effect. Pre-clinical toxicity studies will need to be carried out in a large animal to define doses to be tested in a human clinical trial and to maximize safety. In parallel with the pre-clinical studies leading to a human clinical trial, it will be important to develop the methodology with which to accurately measure the structure and function of the retina of patients with *LCA5* mutations so that the effects of gene therapy in a clinical trial can be captured reliably and accurately. Not only could such studies and a gene therapy clinical trial lead to a treatment for this devastating condition, but they may also provide the framework for assessing the effects of intervention in other severe, early-onset blinding conditions.

Table 3. Cohorts of Neonatal *Lca5*$^{gt/gt}$ Mice Injected at the Designated Post-natal Day and Studied *In Vivo*

	Eye No. 1		Eye No. 2		
Group Number	Testing Material	ROA	Testing Material	ROA	n
Intervention Age: P5					
1	excipient	intravitreal	NA	sham	9
2	excipient	subretinal	NA	sham	11
3	AAV7m8.hopt.*LCA5* (+ 5% AAV7m8.*eGFP*)	intravitreal	NA	sham	18
4	AAV7m8.hopt.*LCA5* + 5% AAV7m8.*eGFP*)	subretinal	NA	sham	25
Intervention Age: P15					
5	excipient	intravitreal	NA	sham	13
6	excipient	subretinal	NA	sham	6
7	AAV7m8.hopt.*LCA5* (+ 5% AAV7m8.*eGFP*)	intravitreal	NA	sham	13
8	AAV7m8.hopt.*LCA5* (+ 5% AAV7m8.*eGFP*)	subretinal	NA	sham	11

ROA, route of administration.

MATERIALS AND METHODS

Experimental Design and Statistical Analysis

Neonatal/juvenile *Lca5*$^{gt/gt}$ (or C57BL/6) littermate controls were chosen randomly to receive unilateral treatment with the test reagent or excipient. The contralateral eyes were used as surgical controls (sham injection). Two to three months after injection, animals were subjected to retinal and visual function tests, and ultimately retinas were studied *ex vivo* or histologically. Statistical analyses differed according to the test paradigm (see below).

Recombinant AAV and *In Vitro* Expression Studies

Recombinant (r)AAV test articles were generated in the CAROT research vector core.[22] A human *LCA5* cDNA was custom-designed for optimal human codon usage (hopt-*LCA5*) and synthesized by DNA2.0 (Menlo Park, CA). The hopt-*LCA5* cDNA was placed under the control of a hybrid CβA promoter, including the CβA exon 1 flanked by intron 1 sequence with a CMV immediate early enhancer (Figure 1A). We selected this constitutive promoter so that we could drive expression not only in photoreceptors but also in other cells in the retina (RPE cells, inner retinal cells, ganglion cells, the lens) that express *LCA5* at various developmental time points.[10] This also allowed us to evaluate any potential toxicity of non-photoreceptor-specific expression of *LCA5*. A bovine growth hormone poly(A) terminator followed the cDNA. A long stuffer sequence was included in the backbone to prevent reverse packaging of the proviral plasmid sequence outside the AAV inverted terminal repeats flanking the transgene cassette. The vectors were made by triple transfection and formulated in excipient consisting of PBS with 0.001% Pluronic F68 (PF68). Reporter vectors incorporated an EGFP cDNA in place of the hopt-*LCA5* cDNA.

The rAAVs were tested for expression of the appropriate sized transgenic Lebercilin protein by western blot analysis. For this, 9.2E+09 − 1.05E+10 vg/μL of AAV7m8.hopt-*LCA5* were delivered into the mouse retina IVT or SR. One month later, retinas were harvested and processed for blotting. Antibodies included an anti-LCA5 rabbit polyclonal antibody (Proteintech, Rosemont, IL), and the signals were quantified, with each value corrected for background and protein loading differences through normalization with a GAPDH immuno-signal.

Lca5$^{gt/gt}$ Mouse Studies

Adult *Lca5*$^{gt/gt}$ mice and C57BL/6 and *Pde6β*$^{-/-}$ (*rd1*, for use as controls in PLR recordings) mice were obtained from Jackson Labs (Bar Harbor, ME). Verification of the genotype of *Lca5*$^{gt/gt}$ animals was performed (Supplemental Materials and Methods). The studies were performed in compliance with federal and institutional regulations on IACUC protocol #805890.

SR injections were carried out unilaterally in post-natal day (P)5 and P15 mice as described previously.[36] IVT injections of AAV7m8 were also carried out (in other cohorts) since this vector had been shown previously to penetrate the mouse retina from the vitreous aspect to target photoreceptors.[22] AAV7m8.CβA.hopt-*LCA5* was injected at a total of 9.2E+09 − 1.05E+10 vg in 1 μL per eye (groups 3, 4, 7, 8; Table 3). The injection solution contained 5% vg/vg of AAV7m8.CβA.eGFP, which served as a transduction reporter. Additional animals received an excipient injection (groups 1, 2, 5, 7; Table 3).

Tests of Retinal/Visual Function

Electroretinography

Mice were anesthetized with a ketamine-xylazine cocktail delivered intramuscularly, their pupils were dilated with 1% tropicamide (Alcon Laboratories, Fort Worth, TX), and the animals were placed on a stage maintained at 37°C. Custom-made clear plastic contact lenses with embedded platinum wires served as recording electrodes, and a platinum wire loop inserted into the animal's mouth served as the reference electrode. ERGs were elicited and recorded with an Espion E2 apparatus (Diagnosys, Lowell, MA). Three ERG responses were recorded under the following settings: scotopic response (dark-adapted animal, 0.01 scot cd s m^{-2} stimulus); maximum rod-cone response (dark-adapted animal, 500 scot cd s m^{-2} stimulus); maximum cone response (30 scot cd m^{-2} adapting steady background light, 500 scot cd s m^{-2} stimulus).

PLR

A Neuroptics (Irvine, CA) A-2000 small animal pupillometer system was used. The amplitudes of pupillary constriction were measured during a series of five light flashes per eye on anesthetized, dark-adapted mice. Flash intensity was 1,000 scotopic lux for 40 ms, a paradigm that did not produce any responses in 1- to 3-month-old rd1 (*Pde6β*$^{-/-}$) mice (data not shown) and thus assured that PLR responses were driven by photoreceptor (but not melanopsin) inputs. PLR amplitude was defined as the difference between the smallest pupil diameter obtained 0.6–1.2 s following the flash stimulus and

the average pupil diameter during 1 s preceding the flash. A criteria response was defined as that pupil contraction that exceeded (>3 SD) the oscillation in pupil diameters during a 1-s pre-interval. A scientist masked to the treatment paradigm evaluated the data from each animal prior to analysis to ensure that each pupil was tracked accurately. If not, that particular animal was excluded from further pupillometry analyses.

Tracked pupil diameters were normalized to the pre-stimulus diameter and the differential value between two eyes at maximal amplitude of the normalized response plot was defined as MDAR (Figure 3G). Higher MDAR values reflect greater responses to intervention. Additional age-matched excipient-injected *Lca5*$^{gt/gt}$ and WT (C57BL/6) mice were used as negative and positive controls, respectively. The MDARs of control *Lca5*$^{gt/gt}$ and C57BL/6 mice were ~0, since there was minimal difference between the two eyes. Statistical analyses employed the two-group t test for comparisons between each treated group and control group or WT group.

Light-Cued Water Maze Navigation Study

Water maze testing was performed to evaluate each animal's ability to see and navigate to a light source, which the animal had been trained to associate with a submerged platform in a five-chamber water maze (Figure S3A; Supplemental Materials and Methods). The light source in the compartment with the platform was a strip with 3 green, with 520 nm emission maximum (901-SB-0465-CT, Mouser Electronics, Mansfield, TX, 1.57E+06 scot cd m^{-2} individual LED luminance). The LED lights emitted negligible heat (Supplemental Materials and Methods). Nevertheless, a transparent, heat-absorbing shield (Edmund Optics, Barrington, NJ) was placed over the LED light panel. Testing was carried out for 4 days using the same procedure used in training but with a series of filters to further dim the light, the two group t test was used for comparison of mean success rate (defined percent of pass trials among all trials of a mouse tested at a specific light intensity) between treated group versus control groups. Statistical analyses using one-way ANOVA.

MEA

We selected MEA testing as a means of analyzing electrophysiological changes in specific regions of the experimental and control retinas, as this allows detailed and quantitative analyses of physiologic responses of multiple single-treated (or control) cells. MEA testing was carried out on five animals 2.5–3.5 months after they had received unilateral IVT injections with AAV7m8.CβA.hopt-*LCA5*. Contralateral eyes were sham-injected and used as negative controls. Four age-matched WT C57BL/6 mice served as positive controls. One outlier WT retina with fast strong response to the first flash and much smaller responses to the following flashes at brighter intensities was removed from the analysis. Retinas from dark-adapted mice were dissected under red light and mounted ganglion cell-side-down in the perforated MEA chamber using modifications of the method previously described.[19,37] Calibrated full-field flashes of 455 nm (efficiency of pigment excitation ~60%, rhodopsin; ~50%, M-opsin; ~0.3%, S-opsin) at different intensities were used for light stimulation (2 s flashes at 0.1 Hz or 50 ms flashes at 4 Hz). Data were analyzed using custom code in MATLAB (MATLAB, Natick, MA); spike sorting was performed in Plexon Offline Sorter (Plexon, Dallas, TX).

Ocular Histology, Histopathology, Immunofluorescence, and TUNEL Assay

Animals were euthanized at 3 months of age. Eyes were enucleated and retinal sections evaluated by modifications of methods previously described.[19] For immunofluorescence studies, sections were incubated with anti-LCA5 (1:300, Proteintech) in the presence of blocking solution, washed, and then incubated with Alexa Fluor 594 conjugated anti-rabbit immunoglobulin G (IgG) secondary antibody (1:500, Invitrogen). Additional antibodies are described in the Supplemental Materials and Methods. TUNEL assay was carried out following manufacturer's recommendations (C10618, Molecular Probes). Sections were imaged with a Zeiss Axio Imager M2 microscope equipped with epifluorescence and Axio-Vision 4.6 software or with a confocal laser-scanning microscope (Leica TCS SP8) equipped with LAS X software. Transmission electron microscopy (TEM) was carried out on designated tissue samples using a JEOL TEM 1010 (JEOL, USA).

Human Studies: PLR Testing

Testing was carried out on a human subject with confirmed homozygous *LCA5* mutations after obtaining written informed consent from an institutional review board (IRB)-approved protocol (#815348). Pupil responses were recorded simultaneously in both eyes with a Procyon P3000 pupillometer and PupilFit6 software (Monmouthshire, UK). Pupillary responses to light were recorded after presentation of 10 lux green light stimuli to the right eye for 0.2 s followed by dark intervals. An infrared-sensitive camera that captured video images at 25 frames/s allowed the pupil diameter of both eyes to be measured every 40 ms.

iPSC Models of *LCA5* Disease

Peripheral blood monocytes (PBMCs) were collected after signed informed consent (IRB approved protocol 808828) from a female proband, JB342, homozygous for *LCA5* mutations p.(Gln279*) (c.835C > T). The unaffected normal-sighted control cells were from individual CHOPWT9. Details of iPSC generation and studies are described in the Supplemental Materials and Methods.

SUPPLEMENTAL INFORMATION

Supplemental Information includes Supplemental Materials and Methods, Supplemental Results, twelve figures, and one table and can be found with this article online at https://doi.org/10.1016/j.ymthe.2018.03.015.

AUTHOR CONTRIBUTIONS

J.Y.S., P.A., S.N., L.L., A.L., J.L.B., J.P., Z.W., I.S., P.H., D.J.B., N.C., J.P., A.M.M., S.Z., T.S.A., J.d.M., J.M., and J.B. participated in the acquisition and/or analysis of data. J.Y.S., P.A., S.N., L.L., A.L., J.L.B., A.M.M., A.I.d.H., F.P.M.C., R.K.K., R.R., P.N., W.P., G.-s.Y., T.S.A., J.d.M., J.M., I.M., J.S., and J.B. participated in the design

and/or interpretation of the reported experiments or results. A.M.M., T.S.A., and J.B. carried out the clinical and research procedures. J.B. and J.P. obtained regulatory approvals. J.Y.S., J.d.M., and J.B. participated in drafting and/or revising the manuscript. J.B. wrote the manuscript, and all other authors reviewed and edited the intermediate and final versions of the manuscript.

CONFLICTS OF INTEREST

J.B. is a founder of Gensight Biologics and of Limelight Bio and a scientific (non-equity-holding) founder of Spark Therapeutics. J.S. is a founder of Limelight Bio. J.B. holds Sponsored Research Agreements (SRAs) from Biogen, Limelight Bio, and REGENXBio and holds a service agreement with Harvard/Astellas. A.M.M. holds Clinical Trial Agreements (CTAs) from Spark Therapeutics. J.L.B., J.S., and J.B. hold intellectual property on a proviral plasmid relevant to this study.

ACKNOWLEDGMENTS

We thank the Brint and Schwartz families for their support of this project, Laura Bryant for assisting with sequence analysis of the human LCA5 cDNA, and Pyroja Sulaiman, PhD, for initial work involving generation of the WT LCA5 cDNA. This study was funded by a Center grant from the Foundation Fighting Blindness to the CHOP-Penn Pediatric Center for Retinal Degenerations, the Brenda and Matthew Shapiro Stewardship, the Robert and Susan Heidenberg Investigative Research Fund for Ocular Gene Therapy, National Eye Institute/NIH grants 1R24 EY019861-01A1 and 8DP1EY023177, Core Grant for Vision Research P30 EY001583, Research to Prevent Blindness, the Paul and Evanina Mackall Foundation Trust, the Center for Advanced Retinal and Ocular Therapeutics, and the F.M. Kirby Foundation. R.K.K. is funded by FFB-Canada and CIHR.

REFERENCES

1. Redmond, T.M., Yu, S., Lee, E., Bok, D., Hamasaki, D., Chen, N., Goletz, P., Ma, J.X., Crouch, R.K., and Pfeifer, K. (1998). Rpe65 is necessary for production of 11-cis-vitamin A in the retinal visual cycle. Nat. Genet. *20*, 344–351.

2. Redmond, T.M., and Hamel, C.P. (2000). Genetic analysis of RPE65: from human disease to mouse model. Methods Enzymol. *316*, 705–724.

3. Maguire, A.M., High, K.A., Auricchio, A., Wright, J.F., Pierce, E.A., Testa, F., Mingozzi, F., Bennicelli, J.L., Ying, G.S., Rossi, S., et al. (2009). Age-dependent effects of RPE65 gene therapy for Leber's congenital amaurosis: a phase 1 dose-escalation trial. Lancet *374*, 1597–1605.

4. Bennett, J., Wellman, J., Marshall, K.A., McCague, S., Ashtari, M., DiStefano-Pappas, J., Elci, O.U., Chung, D.C., Sun, J., Wright, J.F., et al. (2016). Safety and durability of effect of contralateral-eye administration of AAV2 gene therapy in patients with childhood-onset blindness caused by RPE65 mutations: a follow-on phase 1 trial. Lancet *388*, 661–672.

5. Jacobson, S.G., Cideciyan, A.V., Ratnakaram, R., Heon, E., Schwartz, S.B., Roman, A.J., Peden, M.C., Aleman, T.S., Boye, S.L., Sumaroka, A., et al. (2012). Gene therapy for leber congenital amaurosis caused by RPE65 mutations: safety and efficacy in 15 children and adults followed up to 3 years. Arch. Ophthalmol. *130*, 9–24.

6. Bainbridge, J.W., Smith, A.J., Barker, S.S., Robbie, S., Henderson, R., Balaggan, K., Viswanathan, A., Holder, G.E., Stockman, A., Tyler, N., et al. (2008). Effect of gene therapy on visual function in Leber's congenital amaurosis. N. Engl. J. Med. *358*, 2231–2239.

7. Banin, E., Bandah-Rozenfeld, D., Obolensky, A., Cideciyan, A.V., Aleman, T.S., Marks-Ohana, D., Sela, M., Boye, S., Sumaroka, A., Roman, A.J., et al. (2010). Molecular anthropology meets genetic medicine to treat blindness in the North African Jewish population: human gene therapy initiated in Israel. Hum. Gene Ther. *21*, 1749–1757.

8. Weleber, R.G., Pennesi, M.E., Wilson, D.J., Kaushal, S., Erker, L.R., Jensen, L., McBride, M.T., Flotte, T.R., Humphries, M., Calcedo, R., et al. (2016). Results at 2 years after gene therapy for RPE65-deficient Leber congenital amaurosis and severe early-childhood-onset retinal dystrophy. Ophthalmology *123*, 1606–1620.

9. Russell, S., Bennett, J., Wellman, J.A., Chung, D.C., Yu, Z.F., Tillman, A., Wittes, J., Pappas, J., Elci, O., McCague, S., et al. (2017). Efficacy and safety of voretigene neparvovec (AAV2-hRPE65v2) in patients with RPE65-mediated inherited retinal dystrophy: a randomised, controlled, open-label, phase 3 trial. Lancet *390*, 849–860.

10. den Hollander, A.I., Koenekoop, R.K., Mohamed, M.D., Arts, H.H., Boldt, K., Towns, K.V., Sedmak, T., Beer, M., Nagel-Wolfrum, K., McKibbin, M., et al. (2007). Mutations in LCA5, encoding the ciliary protein lebercilin, cause Leber congenital amaurosis. Nat. Genet. *39*, 889–895.

11. Gerber, S., Hanein, S., Perrault, I., Delphin, N., Aboussair, N., Leowski, C., Dufier, J.L., Roche, O., Munnich, A., Kaplan, J., and Rozet, J.M. (2007). Mutations in LCA5 are an uncommon cause of Leber congenital amaurosis (LCA) type II. Hum. Mutat. *28*, 1245.

12. Chen, X., Sheng, X., Sun, X., Zhang, Y., Jiang, C., Li, H., Ding, S., Liu, Y., Liu, W., Li, Z., and Zhao, C. (2016). Next-generation sequencing extends the phenotypic spectrum for LCA5 mutations: novel LCA5 mutations in cone dystrophy. Sci. Rep. *6*, 24357.

13. Corton, M., Avila-Fernandez, A., Vallespín, E., López-Molina, M.I., Almoguera, B., Martín-Garrido, E., Tatu, S.D., Khan, M.I., Blanco-Kelly, F., Riveiro-Alvarez, R., et al. (2014). Involvement of LCA5 in Leber congenital amaurosis and retinitis pigmentosa in the Spanish population. Ophthalmology *121*, 399–407.

14. Vallespin, E., Avila-Fernandez, A., Almoguera, B., Cantalapiedra, D., Garcia-Hoyos, M., Riveiro-Alvarez, R., Aguirre-Lamban, J., Bustamante-Aragones, A., Trujillo-Tiebas, M.J., and Ayuso, C. (2010). Novel human pathological mutations. Gene symbol: LCA5. Disease: Leber congenital amaurosis (LCA). Hum. Genet. *127*, 118.

15. Mackay, D.S., Borman, A.D., Sui, R., van den Born, L.I., Berson, E.L., Ocaka, L.A., Davidson, A.E., Heckenlively, J.R., Branham, K., Ren, H., et al.; [LCA5 Study Group (see acknowledgements for Universities) (2013). Screening of a large cohort of leber congenital amaurosis and retinitis pigmentosa patients identifies novel LCA5 mutations and new genotype-phenotype correlations. Hum. Mutat. *34*, 1537–1546.

16. Ahmad, A., Daud, S., Kakar, N., Nürnberg, G., Nürnberg, P., Babar, M.E., Thoenes, M., Kubisch, C., Ahmad, J., and Bolz, H.J. (2011). Identification of a novel LCA5 mutation in a Pakistani family with Leber congenital amaurosis and cataracts. Mol. Vis. *17*, 1940–1945.

17. Seong, M.W., Kim, S.Y., Yu, Y.S., Hwang, J.M., Kim, J.Y., and Park, S.S. (2009). LCA5, a rare genetic cause of leber congenital amaurosis in Koreans. Ophthalmic Genet. *30*, 54–55.

18. Jacobson, S.G., Aleman, T.S., Cideciyan, A.V., Sumaroka, A., Schwartz, S.B., Windsor, E.A., Swider, M., Herrera, W., and Stone, E.M. (2009). Leber congenital amaurosis caused by Lebercilin (LCA5) mutation: retained photoreceptors adjacent to retinal disorganization. Mol. Vis. *15*, 1098–1106.

19. Boldt, K., Mans, D.A., Won, J., van Reeuwijk, J., Vogt, A., Kinkl, N., Letteboer, S.J., Hicks, W.L., Hurd, R.E., Naggert, J.K., et al. (2011). Disruption of intraflagellar protein transport in photoreceptor cilia causes Leber congenital amaurosis in humans and mice. J. Clin. Invest. *121*, 2169–2180.

20. Vandenberghe, L.H., Bell, P., Maguire, A.M., Cearley, C.N., Xiao, R., Calcedo, R., Wang, L., Castle, M.J., Maguire, A.C., Grant, R., et al. (2011). Dosage thresholds for AAV2 and AAV8 photoreceptor gene therapy in monkey. Sci. Transl. Med. *3*, 88ra54.

21. Ramachandran, P.S., Lee, V., Wei, Z., Song, J.Y., Casal, G., Cronin, T., Willett, K., Huckfeldt, R., Morgan, J.I., Aleman, T.S., et al. (2016). Evaluation of dose and safety of AAV7m8 and AAV8BP2 in the non-human primate retina. Hum. Gene Ther. *28*, 154–167.

22. Dalkara, D., Byrne, L.C., Klimczak, R.R., Visel, M., Yin, L., Merigan, W.H., Flannery, J.G., and Schaffer, D.V. (2013). In vivo-directed evolution of a new adeno-associated virus for therapeutic outer retinal gene delivery from the vitreous. Sci. Transl. Med. *5*, 189ra76.

23. Lyubarsky, A.L., and Pugh, E.N., Jr. (1996). Recovery phase of the murine rod photoresponse reconstructed from electroretinographic recordings. J. Neurosci. *16*, 563–571.

24. Daniele, L.L., Lillo, C., Lyubarsky, A.L., Nikonov, S.S., Philp, N., Mears, A.J., Swaroop, A., Williams, D.S., and Pugh, E.N., Jr. (2005). Cone-like morphological, molecular, and electrophysiological features of the photoreceptors of the Nrl knockout mouse. Invest. Ophthalmol. Vis. Sci. *46*, 2156–2167.

25. Nikonov, S.S., Daniele, L.L., Zhu, X., Craft, C.M., Swaroop, A., and Pugh, E.N., Jr. (2005). Photoreceptors of Nrl -/- mice coexpress functional S- and M-cone opsins having distinct inactivation mechanisms. J. Gen. Physiol. *125*, 287–304.

26. Nikonov, S.S., Kholodenko, R., Lem, J., and Pugh, E.N., Jr. (2006). Physiological features of the S- and M-cone photoreceptors of wild-type mice from single-cell recordings. J. Gen. Physiol. *127*, 359–374.

27. Daniele, L.L., Insinna, C., Chance, R., Wang, J., Nikonov, S.S., and Pugh, E.N., Jr. (2011). A mouse M-opsin monochromat: retinal cone photoreceptors have increased M-opsin expression when S-opsin is knocked out. Vision Res. *51*, 447–458.

28. Xu, J., Dodd, R.L., Makino, C.L., Simon, M.I., Baylor, D.A., and Chen, J. (1997). Prolonged photoresponses in transgenic mouse rods lacking arrestin. Nature *389*, 505–509.

29. Cereso, N., Pequignot, M.O., Robert, L., Becker, F., De Luca, V., Nabholz, N., Rigau, V., De Vos, J., Hamel, C.P., and Kalatzis, V. (2014). Proof of concept for AAV2/5-mediated gene therapy in iPSC-derived retinal pigment epithelium of a choroideremia patient. Mol. Ther. Methods Clin. Dev. *1*, 14011.

30. Parfitt, D.A., Lane, A., Ramsden, C.M., Carr, A.J., Munro, P.M., Jovanovic, K., Schwarz, N., Kanuga, N., Muthiah, M.N., Hull, S., et al. (2016). Identification and correction of mechanisms underlying inherited blindness in human iPSC-derived optic cups. Cell Stem Cell *18*, 769–781.

31. Schwarz, N., Carr, A.J., Lane, A., Moeller, F., Chen, L.L., Aguilà, M., Nommiste, B., Muthiah, M.N., Kanuga, N., Wolfrum, U., et al. (2015). Translational read-through of the RP2 Arg120stop mutation in patient iPSC-derived retinal pigment epithelium cells. Hum. Mol. Genet. *24*, 972–986.

32. Bennett, J. (2017). Taking stock of retinal gene therapy: looking back and moving forward. Mol. Ther. *25*, 1076–1094.

33. Mohamed, M.D., Topping, N.C., Jafri, H., Raashed, Y., McKibbin, M.A., and Inglehearn, C.F. (2003). Progression of phenotype in Leber's congenital amaurosis with a mutation at the LCA5 locus. Br. J. Ophthalmol. *87*, 473–475.

34. Ashtari, M., Cyckowski, L.L., Monroe, J.F., Marshall, K.A., Chung, D.C., Auricchio, A., Simonelli, F., Leroy, B.P., Maguire, A.M., Shindler, K.S., and Bennett, J. (2011). The human visual cortex responds to gene therapy-mediated recovery of retinal function. J. Clin. Invest. *121*, 2160–2168.

35. Bennett, J., Ashtari, M., Wellman, J., Marshall, K.A., Cyckowski, L.L., Chung, D.C., McCague, S., Pierce, E.A., Chen, Y., Bennicelli, J.L., et al. (2012). AAV2 gene therapy readministration in three adults with congenital blindness. Sci. Transl. Med. *4*, 120ra15.

36. Liang, F.-Q., Anand, V., Maguire, A.M., and Bennett, J. (2000). Intraocular delivery of recombinant virus. In Methods in Molecular Medicine: Ocular Molecular Biology Protocols, *Volume 47*, P.E. Rakoczy, ed. Methods in Molecular Medicine: Ocular Molecular Biology Protocols (Humana Press), pp. 125–139.

37. Gaub, B.M., Berry, M.H., Holt, A.E., Reiner, A., Kienzler, M.A., Dolgova, N., Nikonov, S., Aguirre, G.D., Beltran, W.A., Flannery, J.G., and Isacoff, E.Y. (2014). Restoration of visual function by expression of a light-gated mammalian ion channel in retinal ganglion cells or ON-bipolar cells. Proc. Natl. Acad. Sci. USA *111*, E5574–E5583.